

The public reporting burden for this collection of information is estimated to average 1 hour per response, including the time for reviewing instructions, searching existing data sources, gathering and maintaining the data needed, and completing and reviewing the collection of information. Send comments regarding this burden estimate or any other aspect of this collection of information, including suggestions for reducing this burden, to Washington Headquarters Services, Directorate for Information Operations and Reports, 1215 Jefferson Davis Highway, Suite 1204, Arlington VA, 22202-4302. Respondents should be aware that notwithstanding any other provision of law, no person shall be subject to any penalty for failing to comply with a collection of information if it does not display a currently valid OMB control number.
PLEASE DO NOT RETURN YOUR FORM TO THE ABOVE ADDRESS.

1. REPORT DATE (DD-MM-YYYY) 09-04-2014	2. REPORT TYPE Final Report	3. DATES COVERED (From - To) 7-Jun-2009 - 30-Sep-2013
---	--------------------------------	--

4. TITLE AND SUBTITLE Mixing, Combustion, and Other Interface Dominated Flows; Paragraphs 3.2.1 A,B,C and 3.2.2 A	5a. CONTRACT NUMBER W911NF-09-1-0306
	5b. GRANT NUMBER
	5c. PROGRAM ELEMENT NUMBER 611102

6. AUTHORS James Glimm, Xiaolin Li, Xiangmin Jiao, Roman Samulyak	5d. PROJECT NUMBER
	5e. TASK NUMBER
	5f. WORK UNIT NUMBER

7. PERFORMING ORGANIZATION NAMES AND ADDRESSES Research Foundation of SUNY at Stony Brc Office of Sponsored Programs W-5510 Melville Library Stony Brook, NY 11794 -3362	8. PERFORMING ORGANIZATION REPORT NUMBER
--	--

9. SPONSORING/MONITORING AGENCY NAME(S) AND ADDRESS (ES) U.S. Army Research Office P.O. Box 12211 Research Triangle Park, NC 27709-2211	10. SPONSOR/MONITOR'S ACRONYM(S) ARO
	11. SPONSOR/MONITOR'S REPORT NUMBER(S) 54161-MA.48

12. DISTRIBUTION AVAILABILITY STATEMENT Approved for Public Release; Distribution Unlimited
--

13. SUPPLEMENTARY NOTES The views, opinions and/or findings contained in this report are those of the author(s) and should not be construed as an official Department of the Army position, policy or decision, unless so designated by other documentation.

14. ABSTRACT Our progress has focused on advanced numerical algorithms and supporting mathematical theory, with a concentration on higher order geometry in the description of sharp interfaces, stochastic issues in modeling and simulation, and nonlinearities caused by high levels of deformation in the coupling of fluid to solid codes. These general themes are addressed within the context of ARO interests, including parachute drop, brittle fracture, turbulent modeling and turbulent combustion. We developed a new formulation and interpretation of convergence for turbulent combustion simulations with a new rigorous mathematical analysis of turbulent flow. We modeled the

15. SUBJECT TERMS Brittle fracture, parachute drop, fluid material interaction, unstructured grids, surface geometry, turbulence, turbulent combustion

16. SECURITY CLASSIFICATION OF:	17. LIMITATION OF ABSTRACT	15. NUMBER OF PAGES	19a. NAME OF RESPONSIBLE PERSON
a. REPORT UU	UU		James Glimm
b. ABSTRACT UU	UU		19b. TELEPHONE NUMBER 631-632-8370
c. THIS PAGE UU			

Report Title

Mixing, Combustion, and Other Interface Dominated Flows; Paragraphs 3.2.1 A,B,C and 3.2.2 A

ABSTRACT

Our progress has focused on advanced numerical algorithms and supporting mathematical theory, with a concentration on higher order geometry in the description of sharp interfaces, stochastic issues in modeling and simulation, and nonlinearities caused by high levels of deformation in the coupling of fluid to solid codes. These general themes are addressed within the context of ARO interests, including parachute drop, brittle fracture, turbulent modeling and turbulent combustion. We developed a new formulation and interpretation of convergence for turbulent combustion simulations with a new rigorous mathematical analysis of turbulent flow. We modeled the parachute drop both in the later unfolding stages and the free fall stage, with good agreement to experiment and benchmark simulations. We obtained a new mesoscale algorithm for the analysis of brittle fracture and derived a new theoretical analysis of the normal force on a stretched elastic surface.

Enter List of papers submitted or published that acknowledge ARO support from the start of the project to the date of this printing. List the papers, including journal references, in the following categories:

(a) Papers published in peer-reviewed journals (N/A for none)

<u>Received</u>	<u>Paper</u>
09/04/2012 17.00	Xiangmin Jiao, Duo Wang. Reconstructing high-order surfaces for meshing, Engineering with Computers, (09 2011): 0. doi: 10.1007/s00366-011-0244-8
09/06/2011 2.00	W. Bo, X. Liu, J. Glimm, X. Li. A Robust Front Tracking Method: Verification and Application to Simulation of the Primary Breakup of a Liquid Jet, SIAM Journal on Scientific Computing, (07 2011): 1505. doi:
09/06/2011 8.00	H. Lim, J. Iwerks, Y. Yu, J. Glimm, D. H. Sharp. Verification and validation of a method for the simulation of turbulent mixing , Physica Scripta, (12 2010): 14014. doi:
09/06/2011 6.00	X. Li, J. Glimm, X. Jiao, C. Peyser, Y. Zhao. Study of Crystal Growth And Solute Precipitation Through Front Tracking Method, Acta Mathematica Scientia, (03 2010): 377. doi:
09/06/2011 5.00	T. Kaman, H. Lim, Y. Yu, D. Wang, Y. Hu, J.D. Kim, Y. Li, L. Wu, J. Glimm, X. Jiao, X. Li, R. Samulyak. A Numerical Method for the Simulation of Turbulent Mixing and its Basis in Mathematical Theory, Lecture Notes on Numerical Methods for Hyperbolic Equations: Short Course Book, (05 2011): 105. doi:
09/06/2011 3.00	T. Kaman, J. Glimm, D. H. Sharp. Initial Conditions for Turbulent Mixing Simulations, Condensed Matter Physics , (12 2010): 43401. doi:
09/07/2011 9.00	H. Lim, Y. Yu, J. Glimm, X. L. Li, D.H. Sharp. Subgrid Models for Mass and Thermal Diffusion in Turbulent Mixing, Physica Scripta, (12 2010): 14062. doi:
09/07/2011 11.00	H. Lim, Y. Yu, J. Glimm, D. H. Sharp. Nearly Discontinuous Chaotic Mixing , High Energy Density Physics, (01 2010): 223. doi:
09/07/2011 10.00	H. Lim, Y. Yu, J. Glimm, D. H. Sharp. Mathematical, Physical and Numerical Principles Essential for Models of Turbulent Mixing , IMA Volumes in Mathematics and its Applications, (04 2011): 405. doi:
12/18/2013 29.00	Navamita Ray, Duo Wang, Xiangmin Jiao, James Glimm. High-Order Numerical Integration over Discrete Surfaces, SIAM Journal on Numerical Analysis, (01 2012): 0. doi: 10.1137/110857404
12/18/2013 36.00	Gianluca Iaccarino, David Sharp, James Glimm. Quantification of margins and uncertainties using multiple gates and conditional probabilities, Reliability Engineering & System Safety, (06 2013): 0. doi: 10.1016/j.ress.2012.11.026
12/19/2013 34.00	Gui-Qiang Chen, James Glimm. Kolmogorov's Theory of Turbulence and Inviscid Limit of the Navier-Stokes Equations in \mathbb{R}^3 , Communications in Mathematical Physics, (01 2012): 0. doi: 10.1007/s00220-011-1404-9
TOTAL:	12

(b) Papers published in non-peer-reviewed journals (N/A for none)

<u>Received</u>	<u>Paper</u>
09/06/2011 7.00	H. Lim, J. Iwerks, J. Glimm, D. H. Sharp. Nonideal Rayleigh-Taylor Mixing , PNAS, (07 2010): 12786. doi:
09/06/2012 24.00	D.H._Sharp, T._Kaman, H._Lim, J._Glimm. A Mathematical Theory for (LES) Convergence, Philosophical Transactions of the Royal Society - A, (01 2012): 237. doi:
09/06/2012 25.00	T._Kaman, J._Melvin, P._Rao, R._Kaufman, H._Lim, Y._Yu, J._Glimm, D.H._Sharp. Recent Progress in Turbulent Mixing, Physica Scripta, (01 2012): 0. doi:
11/25/2013 28.00	Yan Li,, Xiaolin Li, Joung-Dong Kim,. Simulation of parachute FSI using the front tracking method, Journal of Fluids and Structures, (02 2013): 100. doi:
12/16/2013 31.00	H.K. Lim, Y. Zhou, V.F. de Almeida, J. Glimm. A QMU approach for characterizing the operability limit of air-breathing hypersonic vehicles, , (06 2015): 0. doi:
12/16/2013 32.00	D. Wang, X. Jiao, R. Conley, J. Glimm. On the curvature effect of thin membranes, Journal of Computational Physics, (09 2012): 449. doi:
12/18/2013 43.00	J. Melvin, P. Rao, R. Kaufman, H. Lim, Y. Yu, J. Glimm, D.H. Sharp. Atomic scale mixing for inertial confinement fusion associated hydro instabilities, High Energy Density Physics, (01 2013): 0. doi:
TOTAL:	7

Number of Papers published in non peer-reviewed journals:

(c) Presentations

- 1) "Development of FrontTier++ and Application to Three Problems", Columbia University, New York, October 4, 2013.
- 2) "Numerical Simulation of Parachute", Research Presentation, US Air Force Edwards AFB, June 17, 2013.
- 3) "Front tracking on Fabric Modeling and Application to Parachute Dynamics", Wuhuan Institute of Physics, Chinese Academia Sinica, July 6, 2012.
- 4) "Front Tracking and Application in Fluid Physics", Departmental Colloquium, Beijing Normal University, July 4, 2012.
- 5) "Front Tracking on Fabric Modeling and Application to Parachute Dynamics", Department Colloquium, Shanghai Jiaotong University, July 3, 2012.
- 6) "Lagrangian Front Tracking Method to Fluid Instability Problems", Xiaolin Li, Department of Mathematics, National Taiwan University, Taipei, March 19, 2012.
- 7) "A Spring Model and the ODE System for the Study of Fabric Surface and Its Application in Parachute Simulation", Xiaolin Li, Joung-Dong Kim, and Yan Li, Department of Mathematics, National Sun Yat-sen University, Kaohsiung, Taiwan, March 21, 2012.
- 10) "Front Tracking Method and Applications to Fabric Modeling and Parachute Simulation", Xiaolin Li, Joung-Dong Kim, and Yan Li, Department of Mathematics, National Cheng Kung University, Tainan, Taiwan, March 22, 2012.
- 11) "Mathematics and Applications", Sanya College, China, 4/18-4/22, 2011.
- 12) "Recent development of the front tracking method and some new applications", Institute of Applied Physics and Computational Mathematics, Beijing, China, July 16, 2010.
- 13) "Front tracking on Convection Dominated Problems", Peking University, Beijing, China, June 16, 2010.
- 14) "Supercomputing and front tracking method", Wuhan University, Wuhan, China, June 21, 2010.
- 15) "Front tracking and interfacial physics", Wuhan Institute of Physics, Academia Sinica, Wuhan, China, June 22, 2010.
- 16) "Partial differential equations and free boundary problems", Linyi Normal University, Linyi, China, June 28, 2010.
- 17) "Front tracking and convection dominated problems", Zhejiang University, Hangzhou, China, July 8, 2010.
- 18) "Surface Mesh Optimization and Adaption with High-Order Accuracy, Advances in Computational Mechanics", Navamita Ray, Tristan Delaney, Xiangmin Jiao, San Diego, CA, February 24-27, 2013.
- 19) "A Numerical Method for the Simulation of Turbulent Mixing and its Basis in Mathematical Theory", T. Kaman, H. Lim, Y. Yu, D. Hu, Y. Kim, J.-D. Kim, YI Li, L. Wu, J. Glimm, X. Jiao, X.-L. Li, R. Samulyak, International Conference to honour Professor E.F. Toro, July 4, 2011.
- 20) Front Tracking Method on Precipitation with Subsurface Flow, Yijing Hu, Xiaolin Li, SIAM Conference on Computational Science & Engineering (CSE11), Reno, Nevada, March 3, 2011.
- 21) Lagrangian Front Tracking Method to Fluid Instability Problems, Xiaolin Li, Department of Mathematics, National Taiwan University, Taipei, March 19, 2012.
- 22) A spring Model and the ODE System for the Study of Fabric Surface and Its Application in Parachute Simulation, Xiaolin Li, Joung-Dong Kim, and Yan Li, Department of Mathematics, National Sun Yat-sen University, Kaohsiung, Taiwan, March 21, 2012.
- 23) Front Tracking Method and Applications to Fabric Modeling and Parachute Simulation, Xiaolin Li, Yan Li, I-Liang Chern, Joung-Dong Kim, East Asia SIAM Conference, June 25, 2012.
- 24) Modeling of Airfoil Dynamics with Front Tracking Method, Joung-Dong Kim, Yan Li, and Xiaolin Li, Pusan National University, Republic of Korea, March 12, 2012.
- 25) Simulation of Parachute Inflation Using the Front Tracking Method, Joung-Dong Kim, Yan Li, and Xiaolin Li, Ulsan National Institute of Science and Technology, Republic of Korea, March 20, 2012.
- 26) Modeling of Airfoil Dynamics with Front Tracking Method, Joung-Dong Kim, Yan Li, and Xiaolin Li, National Institute for Mathematical Sciences, Republic of Korea, March 27, 2012.
- 27) Simulation of Parachute FSI Using the Front Tracking Method, Joung-Dong Kim, Yan Li, and Xiaolin Li, University of Arizona, May 22, 2012.
- 28) Front Tracking Method and Its Application in Science and Engineering, Xiaolin Li, Shanghai Jiaotong University, Shanghai, China, July 4, 2012.
- 29) Front Tracking Method and Its Application in Science and Engineering, Xiaolin Li, Beijing Normal University, Beijing, China, July 5, 2012.
- 30) Simulation of Parachute Inflation Using the Front Tracking Method, Joung-Dong Kim, Yan Li, and Xiaolin Li, IAM Annual Meeting, Minneapolis, Minnesota, July 13, 2012.
- 31) James Glimm. October 20, 2010. "Turbulent Mixing for a Jet in Crossflow and Plans for Turbulent Combustion." Poster presentation in PSAAP project meeting, Stanford, CA.
- 32) October 28. "A computer Science Approach to Interface Dominated Fluid Problems." CMACS Project Conference, New York University, NY, November 9, 2010.
- 33) James Glimm. "One Mathematician's View of the Growing Role of Mathematics across Science and Beyond." Stelson Lecture, Georgia Institute of Technology, Atlanta, GA, November 22, 2010.
- 34) James Glimm. "Mathematical, Numerical, and Physical Principles for Turbulent Mixing." Mathematics Colloquium Lecture, Georgia Institute of Technology, Atlanta, GA, November 23, 2010.
- 35) James Glimm. "An Overview of Turbulent Mixing." Computations in Science Lecture, University of Chicago, Chicago, IL, December 8, 2010.
- 36) James Glimm. "Numerical Errors for Solutions of Partial Differential Equations." CMACS Conference Presentation, Lehman College, New York, NY, January 18, 2011.
- 37) James Glimm. "UQ for Turbulent Mixing." Mini-symposium Invited Presentation, SIAM CS&E Conference, Reno, NV, March 4, 2011.
- 38) James Glimm. "Two Phase flow and Applications to Chemical Processing". Mini-symposium Plenary Invited Talk, 16th International

Conference on Finite Elements in Flow Problems, Munich, Germany, March 24, 2011.

39) James Glimm. "Mathematical theories of existence for 3D conservation laws and the nature of convergence in the large eddy simulation regime." Invited talk, Conference on Nonlinear Evolution Equations, Ann Arbor, MI, May 3, 2011.

40) James Glimm. "A numerical method for the simulation of turbulent mixing and its basis in mathematical theory." Short Course on Numerical Methods for Hyperbolic Equations, Santiago de Compostela, Spain, July 4, 2011.

41) James Glimm. "Mathematical theories of existence for 3D conservation laws and the nature of convergence in the large eddy simulation regime." Invited Plenary Lecture, Numerical Methods for Hyperbolic Equations, Theory and Applications, Santiago de Compostela, Spain, July 5, 2011.

42) James Glimm. "Uncertainty Quantification for Turbulent Reacting Flows." Plenary Lecture, Uncertainty Quantification in Scientific Computation NIST, Boulder, CO, August 3, 2011.

43) James Glimm. "LES for Turbulent Mixing and Combustion." Invited lecture, Turbulent Mixing and Beyond, ICTP, Trieste, Italy, August 25, 2011.

44) N. Ray, D. Wang, X. Jiao, and J. Glimm. "High-order Computation of Surface Integrals over Discrete Surfaces." 7th International Congress on Industrial and Applied Mathematics - ICIAM 2011, Vancouver, BC, Canada, July 2011.

45) X. Jiao. "Some Mathematical Issues at Interfaces in Multiphysics Coupling." DOE Multiphysics Workshop, Park City, UT, July 2011.

Number of Presentations: 45.00

Non Peer-Reviewed Conference Proceeding publications (other than abstracts):

<u>Received</u>	<u>Paper</u>
09/05/2012 18.00	Tulin_Kaman, Ryan_Kaufman, James_Glimm, David_H_Sharp. Uncertainty Quantification for Turbulent Mixing Flows: Rayleigh-Taylor Instability, IFIP Advances in Information and Communication Technology. 01-AUG-11, . . . ,
09/06/2011 1.00	T. Kaman, H. Lim, Y. Yu, D. Wang, Y. Hu, J.-D. Kim, Y. Li, L. Wu, J. Glimm, X. Jiao, X.-L. Li, R. Samulyak . A Numerical Method for the Simulation of Turbulent Mixing and its Basis in Mathematical Theory, International Conference to honour Professor E. F .Toro. 04-JUL-11, . . . ,
09/06/2012 23.00	T._Kaman, H._Lim, Y._Yu, D._Wang, Y._Hu, J.-D._Kim, X._Jiao, X.-L._Li, R._Samulyak. A Numerical Method for the Simulation of Turbulent Mixing and its Basis in Mathematical Theory, Proceedings of the 2011 companion on High Performance Computing Networking, Storage and Analysis Companion . 14-NOV-11, . . . ,
12/18/2013 44.00	E. Bartocci, F.H. Fenton, J. Glimm, R.A. Gray, E.M. Cherry, S.A. Smolka, R. Grosu, A. Murthy. Curvature Analysis of Cardiac Excitation Wavefronts, ,
12/20/2013 12.00	R. Samulyak, H. Wei. Mesoscale Models and Algorithms for Fracture of Solids , ASME 2011 Applied Mechanics and Materials Conference. 30-MAY-11, . . . ,
TOTAL:	5

Number of Non Peer-Reviewed Conference Proceeding publications (other than abstracts):

Peer-Reviewed Conference Proceeding publications (other than abstracts):

Received

Paper

09/01/2012 13.00 Bryan Clark, Navamita Ray, Xiangmin Jiao. Surface mesh optimization, adaption and untangling with high-order accuracy, 21st International Meshing Roundtable. 08-OCT-12, . . . ,

12/16/2013 38.00 T. Kaman, H. Lim, Y. Yu, D. Wang, Y. Hu, J.-D. Kim, Y. Li, L. Wu, J. Glimm, X. Jiao, X.-L. Li, R. Samulyak. A Numerical Method for the Simulation of Turbulent Mixing and its Basis in Mathematical Theory†, Numerical Methods for Hyperbolic Equations: Theory and Applications. An international conference to honour Professor E.F. Toro. 04-JUL-11, . . . ,

12/20/2013 40.00 R. Kaufman, T. Kaman, Y. Yu, J. Glimm. wstar Documentation, Proceeding Book of International Conference to honour Professor E.F. Toro. 04-JUL-11, . . . ,

TOTAL: 3

(d) Manuscripts

<u>Received</u>	<u>Paper</u>
09/01/2012 14.00	Duo Wang, Xiangmin Jiao, Rebecca Conley, James Glimm. On the Curvature Effect of Thin Membranes, Journal of Computational Physics (01 2012)
09/02/2012 15.00	Navamita Ray, Duo Wang, Xiangmin Jiao, James Glimm. High-Order Numerical Integration over Discrete Surfaces, SIAM Journal on Numerical Analyses (01 2012)
09/02/2012 16.00	Joung-Dong Kim, Yan Li, Xiaolin Li. Simulation of Parachute FSI Using the Front Tracking Method, Journal of Fluids and Structures (12 2011)
09/06/2012 21.00	J._Melvin, P._Rao, R._Kaufman, H._Lim, Y._Yu, J._Glimm, D.H._Sharp. Atomic Scale Mixing for Inertial Confinement Fusion Associated Hydro Instabilities, High Energy Density Physics (08 2012)
09/06/2012 22.00	J._Glimm, D.H._Sharp, T._Kaman, H._Lim. New Directions for Rayleigh-Taylor Mixing, Philosophical Transactions of the Royal Society - A (04 2012)
12/16/2013 30.00	B. Plohr, J. Glimm, D. Sharp. Large eddy simulation, turbulent transport and the renormalization group, arXiv:1308.3221 (02 2012)
12/16/2013 39.00	T. Kaman, J. Melvin, P. Rao, R. Kaufman, H. Lim, Y. Yu, J. Glimm, D.H. Sharp. Recent Progress in Turbulent Mixing, Physica Scripta (09 2011)
12/16/2013 37.00	T. Kaman, R. Kaufman, J. Glimm, D.H. Sharp. Uncertainty Quantification for Turbulent Mixing Flows: Rayleigh-Taylor Instability, IFIP Advances in Information and Communication Technology (01 2012)
12/16/2013 35.00	D.H. Sharp, T. Kaman, H. Lim, J. Glimm. New Directions for Rayleigh-Taylor Mixing, Royal Society (01 2013)
12/18/2013 42.00	R. Kaufman, H. Lim, T. Kaman, P. Rao, J. Glimm, J. Melvin. Macro and micro issues in turbulent mixing, Science China Technological Sciences (01 2013)
12/18/2013 41.00	H. Lim, T. Kaman, Y. Yu, V. Mahadeo, Y. Xu, H. Zhang, J. Glimm, S. Dutta, D.H. Sharp, B. Plohr. A Mathematical Theory for LES Convergence, Acta Mathematica Scientia (01 2012)
12/19/2013 45.00	Y. Hu, V. F. de Almeida, X. Li. Front Tracking Method on Phase Transition Problems and Applications, Journal of Computational Physics (05 2013)

TOTAL: 12

Number of Manuscripts:

Books

Received Paper

TOTAL:

Patents Submitted

Patents Awarded

Awards

American Mathematical Society inducted Prof. James Glimm to the inaugural class of Fellows of the AMS (2013).

Prof. James Glimm awarded a Galileo medal by the mayor of Padua, Italy during the 2012 International Conference on Hyperbolic Problems and Applications.

Graduate Students

<u>NAME</u>	<u>PERCENT SUPPORTED</u>	Discipline
Hao Zhang	0.12	
Joungdong Kim	1.00	
Ying Xu	0.12	
Yijing Hu	1.00	
Yan Li	1.00	
Wei Li	1.00	
Xinglin Zhao	0.50	
FTE Equivalent:	4.74	
Total Number:	7	

Names of Post Doctorates

<u>NAME</u>	<u>PERCENT SUPPORTED</u>
FTE Equivalent:	
Total Number:	

Names of Faculty Supported

<u>NAME</u>	<u>PERCENT SUPPORTED</u>	National Academy Member
Xiangmin Jiao	0.08	No
Xiaolin Li	0.08	No
FTE Equivalent:	0.16	
Total Number:	2	

Names of Under Graduate students supported

<u>NAME</u>	<u>PERCENT SUPPORTED</u>
FTE Equivalent:	
Total Number:	

Student Metrics

This section only applies to graduating undergraduates supported by this agreement in this reporting period

The number of undergraduates funded by this agreement who graduated during this period: 0.00

The number of undergraduates funded by this agreement who graduated during this period with a degree in science, mathematics, engineering, or technology fields:..... 0.00

The number of undergraduates funded by your agreement who graduated during this period and will continue to pursue a graduate or Ph.D. degree in science, mathematics, engineering, or technology fields:..... 0.00

Number of graduating undergraduates who achieved a 3.5 GPA to 4.0 (4.0 max scale):..... 0.00

Number of graduating undergraduates funded by a DoD funded Center of Excellence grant for Education, Research and Engineering:..... 0.00

The number of undergraduates funded by your agreement who graduated during this period and intend to work for the Department of Defense 0.00

The number of undergraduates funded by your agreement who graduated during this period and will receive scholarships or fellowships for further studies in science, mathematics, engineering or technology fields:..... 0.00

Names of Personnel receiving masters degrees

<u>NAME</u>
Total Number:

Names of personnel receiving PHDs

<u>NAME</u>
Total Number:

Names of other research staff

<u>NAME</u>	<u>PERCENT SUPPORTED</u>
FTE Equivalent:	
Total Number:	

Sub Contractors (DD882)

Inventions (DD882)

Scientific Progress

See Attachment entitled "final-summary-13.pdf" in zip file

Technology Transfer

1. INTRODUCTION

Our work has two main thrusts.

The first thrust is to develop high quality numerical tools for resolution of complex (often stochastic and often dynamic) geometries within a simulation. High order geometry has taken our front tracking code FronTier to a new scientific level. Novel theories of stochastic convergence have been applied to turbulent combustion. A new and very promising method for modeling brittle fracture was developed

The second thrust is to explore the use of these tools in a series of vital, ARO relevant applications: brittle fracture, parachute drop, turbulent combustion and robust finite element methods for unstructured grids.

2. NUMERICAL TOOLS FOR COMPLEX, DYNAMIC GEOMETRY

2.1. Weighted Least Squares over Discrete Surfaces. During this project, we have developed a unified theoretical framework based on the weighted least squares (WLS) framework. The WLS framework is general and subsumes the traditional interpolation-based theoretical foundation. It delivers the same order of accuracy but far superior stability and flexibility on irregular meshes over complex geometries, a fact which we have proven mathematically and demonstrated numerically.

Using the WLS framework, we have addressed some fundamental problems in scientific computing. The first problem is surface integration, which is a core procedure for a variety of numerical methods such as the boundary integral method, finite element method, surface finite elements etc., as well as for the computation of geometrical primitives such as surface area and volume. We addressed the fundamental question of whether one can achieve high-order accuracy given a piecewise linear approximation to the surface. We proposed a novel method, which can compute the surface integrals to high-order of accuracy over piecewise-linear meshes [29, 9]. We proved theoretically that high-order of accuracy can be achieved for surface integrals using a least-squares based approximation over linear meshes and demonstrated numerical experiments achieving the predicted order of accuracy.

2.2. High-Order Surface Remeshing. Surface remeshing is a widely used strategy for a variety of purposes such as mesh quality improvement, conformality to highly curved boundaries, error-based adaptation, etc. The accuracy of geometry can be easily lost if low-order

point projections are used during remeshing operations. We investigated the problem of optimizing, adapting, and untangling a surface triangulation with high-order accuracy, so that the resulting mesh has sufficient accuracy to support high-order numerical methods, such as finite element methods with quadratic or cubic elements or generalized finite difference methods. The fundamental idea to solve this problem was to integrate various remeshing strategies with a high-order point projection. Specifically, we developed a remeshing strategy based on variational mesh optimization along with high-order surface reconstruction that produces high-quality triangular meshes. The algorithm was further improved to allow of untangling mildly folded triangles. These results were reported in [4]. In general, high-order point projection works well for sufficiently resolved regions. However, they may introduce large variations if applied to regions which lie beyond the asymptotic limit of polynomial fittings such as under-resolved regions describing regions of high curvature. We introduced safeguards (also known as limiters) to capture such problematic regions and subsequently reduce the order of fitting, resulting in a robust algorithm [28]. Extensive numerical experiments were performed to demonstrate the effectiveness of our method in obtaining convergent differential quantities as well as comparison to other methods. This work has been integrated in the front-tracking package FronTier.

2.3. Theoretical Model of Curvature Effect of Thin Membranes.

As part of the project, we investigate the curvature effect of a thin, curved elastic interface [47]. Such an interface separates two subdomains, such as the canopy of parachutes, and it exerts a pressure due to a curvature effect. We refer to this pressure as the interface pressure; it is similar to the surface tension in fluid mechanics. It is important in some applications, such as the canopy of parachutes, biological membranes of cells, balloons, airbags, etc., as it partially balances a pressure jump between the two sides of an interface. In this project, we showed that the interface pressure is equal to the trace of the matrix product of the curvature tensor and the Cauchy stress tensor in the tangent plane. We derive the theory for interfaces in both 2-D and 3-D, and present numerical discretizations for computing this quantity over triangulated surfaces. Figure 1 shows an example computation of the curvature effect, where a torus with inner and outer radii 0.3 and 1 m was artificially expanded into one with inner and outer radii 0.32 and 1.05 m. Colors of left and right images indicate the tangential stress and interface pressure, respectively. It can be seen that the stress (and also pressure) is larger at the outside than at the inside. Figure 2 shows

the high-order convergence rates that were achieved of this model when discretized using the weighted least squares framework.

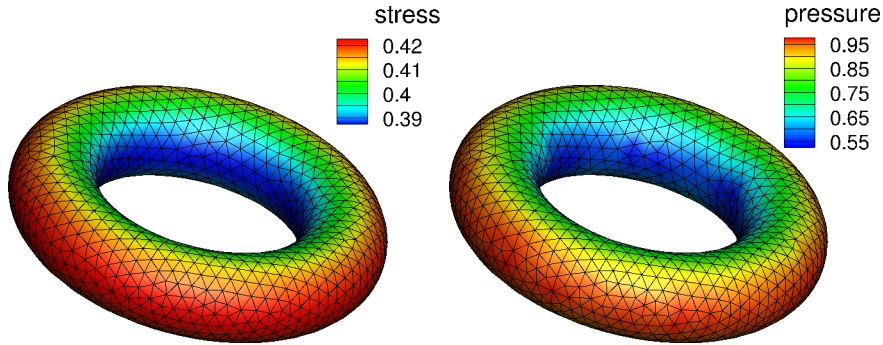


FIGURE 1. An example computation of interface pressure due to curvature effect.

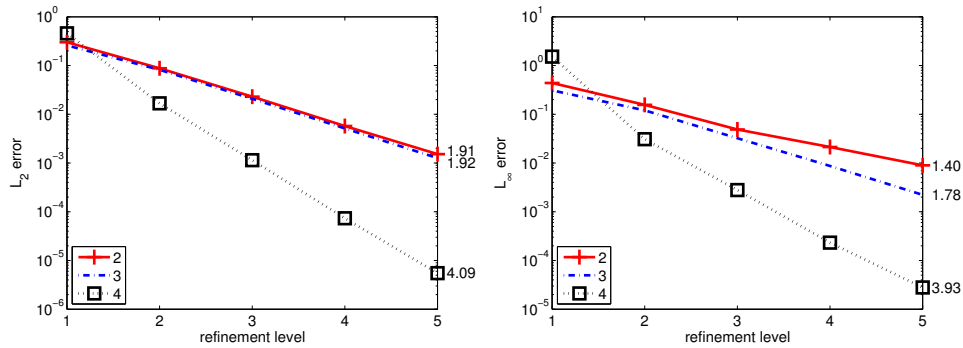


FIGURE 2. High-order convergence results for computed interface pressure under grid refinement for the torus.

3. APPLICATIONS

3.1. Brittle Fracture. We have developed new mathematical models, numerical algorithms and parallel software for the simulation of brittle fracture of solids. The algorithms are based on energy minimization in a network of triangular springs with critical strain and splitting of overstressed bonds. The algorithms ensure conservation of mass during the crack evolution. Special energy penalty terms preclude mesh folding and overlapping in the simulation of compressed materials. The main emphasis of the research was on the study of brittle fracture, but elasto-plastic models for springs have also been developed for the simulation of plastic deformations with limited shear bands.

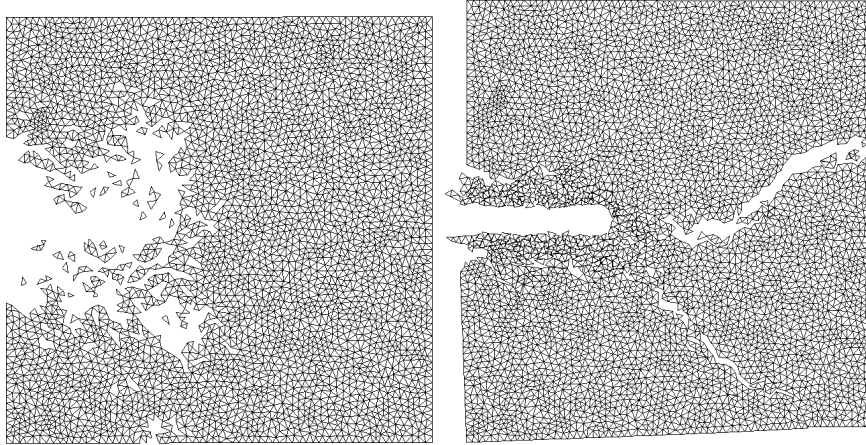


FIGURE 3. Comparison of non-conservative and mass-conservative methods using the example of projectile impact induced wall fracture. Left: the non-conservative method results in large mass loss, with the creation of a large void; Right: The mass conservative method leads to increased pressure and the formation of cracks.

Our models significantly improved similar previous models based on the energy minimization of spring networks. The main deficiencies of prior methods, resolved by our methods, are

- Algorithms applicable only to stretched solids. Unphysical mesh folding occurs if these models are applied to solids under compression forces.
- Non-conservative bond removal algorithm which leads to the loss of mass. This issue is less important if only a small number of isolated cracks develop in stretched solids, but it prevents the simulation of comminuted fracture zones in compressed solids.
- Inability to reproduce complex patterns occurring in brittle fracture processes (for instance a comminuted zone and a series of radial cracks in solid plates hit by high velocity projectiles).
- Only 2D dimensional models
- Serial codes for running on single-processor computers

Our representation of solids by spring networks contains the two degrees of freedom necessary to match real material properties and it exhibits a stable Poisson ratio. Two regimes of the brittle fracture have been considered: adiabatically slow deformation with breakup,

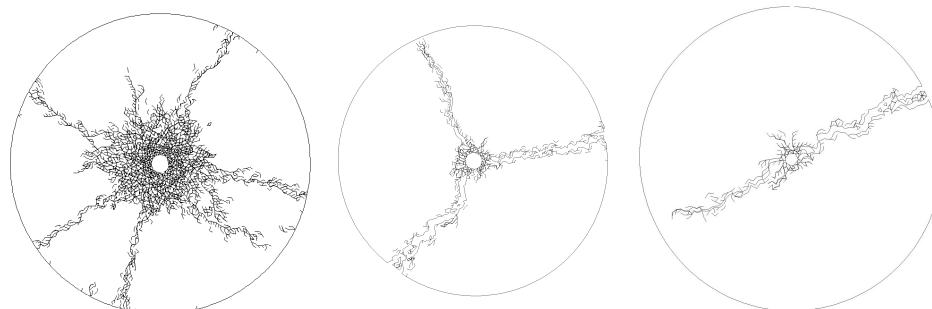


FIGURE 4. Brittle fracture of thin disks hit by projectiles exhibiting comminuted regions and radial cracks. The number of radial cracks and the comminuted region size decrease with the increase of material plasticity and reduction of the projectile velocity.

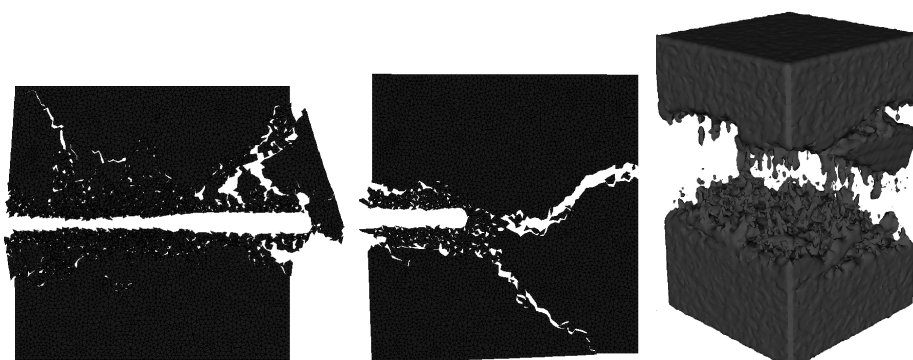


FIGURE 5. Left and center: 2D simulation of brittle fracture of a thick wall hit by a projectile. One-layer of inscribed circles (left) and two-layers of inscribed circles (center) were used in the fragment collision detection algorithm. Right: Fracture of a 3D rod under tension.

and instantaneously fast deformation with the formation and propagation of cracks in stressed materials. Parallel software for the fracture of brittle materials under strain has been developed using the external parallel packages TAO and Global Arrays, developed within DOE high performance computing initiatives. A Schwartz-type overlapping domain decomposition and the corresponding acceleration techniques have also been studied. Three different visualization techniques have been developed to capture details of fractured zones in 3D.

The software has been applied to the simulation of fracture of solids in the regime of

1. slow stretching deformations,
2. materials possessing high initial quasi-stable overstress such as in the rapid disintegration of highly tempered glass in the phenomenon called the Prince Rupert drop, and
3. fracture of thin brittle discs and thick walls hit by high velocity projectiles [48, 49].

The bifurcation of the fracture dynamics from the growth of the comminuted zone to the propagation of isolated radial cracks, typical for the fracture of glass sheets and thin ceramic plates hit by projectiles, has been reproduced in our numerical experiments. Scaling studies involving the variation of material properties and projectile velocity have been performed (see Figure 4). 2D and 3D simulations of the fracture of thick walls are depicted in Figure 5 [48, 49]. The fracture model has also been used in a coupled multiscale simulation of the nuclear fuel rod failure within a study of nuclear reactor safety issues [2, 1].

The main research goal of the present study is to improve the availability of the method by use of a finite elements implementation. This will enable standard finite element codes to simulate complex fracture regimes and flows of disintegrated materials. The related goal is the development of highly scalable software, and applications to problems relevant to Army Research Laboratory and DOE Nuclear Energy research.

3.2. Numerical Modeling of Parachute Delivery System. Simulation of parachute inflation via computational method has attracted the attention of scientists at the Department of Defense laboratories and academia alike. Some of the successful studies include those reported in [34, 33, 30, 35, 31, 32], where the Deforming - Spatial - Domain / Stabilized Space-Time (DSD/SST) method [39, 40] was used in [33, 30, 35, 31, 32]. The studies in [43, 42, 37, 38, 44] also used the DSD/SST as the core numerical method, but involved new versions and special techniques. These studies successfully address the computational challenges in handling the geometric complexities of the parachute canopy and the contact between parachutes in a cluster. Kim and Peskin et al. used the immersed boundary method to study the semi-opened parachute in both two and three dimensions [18, 19], their simulations are on small Reynolds number (about 300) and applied payload with several grams. Karagiozis used the large-eddy simulation to study the parachute in Mach 2 supersonic flow [16]. Purvis [26, 27] used springs to represent the structures of the fore-body, the

suspension lines, and the canopy, etc. In these papers, the authors used cylindrical coordinates with the center line as the axis. In the paper by Strickland et al. [36], the authors developed an algorithm called PURL to couple the structure dynamics (PRESTO) and fluid mechanics (CURL), in which mass is added to each of the structure node based on the diagonally added mass matrix and a pseudo is computed from the fluid code which is the sum of the actual pressure and the pressure associated with the diagonally added mass. Tutt and Taylor [46, 45] simulated the parachute through the LS-DYNA code. They used an Eulerian-Lagrangian penalty coupling algorithm and multi-material ALE capabilities with LS-DYNA to replicate the inflation of small round canopies in a water tunnel.

Our computational approach to the simulation of the parachute delivery system is based on the front tracking platform. In the last ARO funded project during which the PI served as the principal developer, we established a computational platform for the parachute study by employing the spring model for the parachute canopy and the string chords. We designed new data structure to allow the application of the *FronTier* library to the dynamic motion of fabric surface driven by the gravitational force of payload and the fluid pressure. We discretize the fabric surface into a homogeneously triangulated surface mesh.

3.2.1. Analysis of the Spring System. We made a detailed analysis of the spring system which is used to model the fabric surface of the parachute canopy (Figure 6). When no external driving force is applied, the fabric surface, which is represented by the spring mass system, is a conservative system whose total energy (kinetic energy plus potential energy) is a constant. Assuming each mesh point represents a point mass m in the spring system with position vector \mathbf{x}_i , the kinetic energy of the mass point i is $T_i = \frac{1}{2}m|\dot{\mathbf{x}}_i|^2$, where $\dot{\mathbf{x}}_i$ is the time derivative, or velocity vector of the mass point i .

We considered two types of spring systems. The first one, which we refer to as Model-I, or the elastic foil model, has the potential energy between two mass points \mathbf{x}_i and \mathbf{x}_j in the form of

$$V_{ij} = \frac{k}{2} |(\mathbf{x}_i - \mathbf{x}_j) - (\mathbf{x}_{i0} - \mathbf{x}_{j0})|^2, \quad (1)$$

where k is the spring constant and \mathbf{x}_{i0} is the equilibrium position of mass point i . This potential energy leads to the following equation of

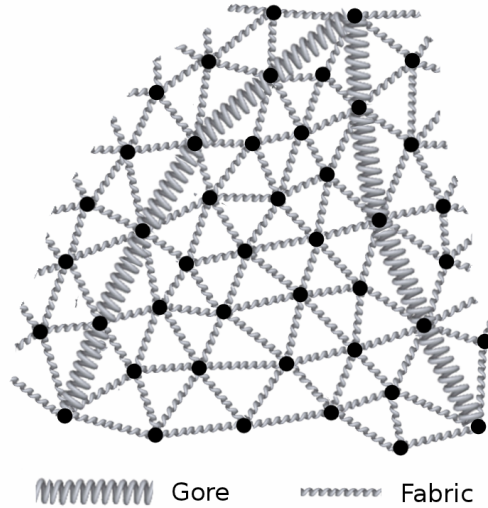


FIGURE 6. The spring model on a triangulated mesh. Each vertex point in the mesh represents a mass point with point mass m . Each edge of the triangles has an equilibrium length set during initialization and the changing length exerts a spring force on the two neighboring vertices in opposite directions. Gores are added as curves with larger spring constant. This plot shows the mesh of canopy with gores.

motion for the system

$$m \frac{d^2 \mathbf{x}_i}{dt^2} + \sum_{j=1}^N \eta_{ij} k ((\mathbf{x}_i - \mathbf{x}_j) - (\mathbf{x}_{i0} - \mathbf{x}_{j0})) = 0, \quad i = 1, 2, \dots, N \quad (2)$$

where \mathbf{x}_{i0} is the equilibrium position of mass point i . This system can be simplified by the substitution $\mathbf{x}'_i = \mathbf{x}_i - \mathbf{x}_{i0}$, $i = 1, 2, \dots, N$, which yield

$$m \frac{d^2 \mathbf{x}'_i}{dt^2} + \sum_{j=1}^N \eta_{ij} k ((\mathbf{x}'_i - \mathbf{x}'_j)) = 0, \quad i = 1, 2, \dots, N \quad (3)$$

This system does not match the properties of fabric, but it can be analyzed in closed form.

Using the Levy-Desplanques Theorem for diagonally dominated matrix, we proved [21] that the motion of Model-I is purely oscillatory and there exists an upper bound for the eigen frequencies of Model-I. In addition, through the Gershgorin circle theorem, we have obtained

an upper bound for the eigen frequency of the oscillatory motion

$$\omega \leq \sqrt{\frac{2Mk}{m}}, \quad (4)$$

A fabric surface is considered as a membrane which is an idealized two dimensional manifold for which forces needed to bend it are negligible. Therefore for parachute canopy, we should not consider the bending energy. Model-I contains strong bending force and is not suitable for fabric modeling. To obtain a realistic spring system for the simulation of fabric surface, we have to assume that the spring force between two neighboring point masses is only proportional to the displacement from their equilibrium distance, the potential energy due to the relative displacement between two neighboring point masses \mathbf{x}_i and \mathbf{x}_j is given by

$$V_{ij} = \frac{k}{2} (|\mathbf{x}_i - \mathbf{x}_j| - l_{ij}^0)^2, \quad (5)$$

where $l_{ij}^0 = |\mathbf{x}_{i0} - \mathbf{x}_{j0}|$ is the equilibrium length between the two point masses. Here we have made a modification to the model used by Choi and Ko in that we allow both contraction and expansion forces while in Choi and Ko's equation, no force is applied if $|\mathbf{x}_i - \mathbf{x}_j| < l_{ij}^0$. Choi and Ko's choice does not conserve energy and would allow a surface to shrink to a point without resistance. Such shrinking is unrealistic for a fabric surface such as the parachute canopy. We refer to this model as Model-II, or the fabric model.

The equation of motion of Model-II can be written as

$$m \frac{d^2 \mathbf{x}_i}{dt^2} = - \sum_{j \neq i} a_{ij}(r_{ij}) (\mathbf{x}_i - \mathbf{x}_j), \quad (6)$$

where

$$a_{ij} = \eta_{ij} k \left(1 - \frac{l_{ij}}{r_{ij}} \right), \quad r_{ij} = |\mathbf{x}_i - \mathbf{x}_j|.$$

Upon linearization, we have

$$m \frac{d^2 \delta \mathbf{x}_i}{dt^2} = - \sum_{j \neq i} \eta_{ij} k \left(\frac{l_{ij}}{r_{ij}} \mathbf{e}_{ij} \otimes \mathbf{e}_{ij} + \left(1 - \frac{l_{ij}}{r_{ij}} \right) I \right) (\delta \mathbf{x}_i - \delta \mathbf{x}_j) \quad (7)$$

Using \mathbf{e}_{ij} to make dot product for each term, we obtain the tangential component of acceleration

$$\begin{aligned} f_{ij}^t &= -\mathbf{e}_{ij} \cdot \eta_{ij} k \left(\frac{l_{ij}}{r_{ij}} \mathbf{e}_{ij} \otimes \mathbf{e}_{ij} + \left(1 - \frac{l_{ij}}{r_{ij}} \right) I \right) (\delta \mathbf{x}_i - \delta \mathbf{x}_j) \\ &= -\eta_{ij} k (\mathbf{e}_{ij} \cdot (\delta \mathbf{x}_i - \delta \mathbf{x}_j)) \end{aligned} \quad (8)$$

This equation indicates that the tangential force of the fabric model (Model-II) is the same as in Model-I. Therefore we conclude that for Model-II, only the tangential motion is oscillatory.

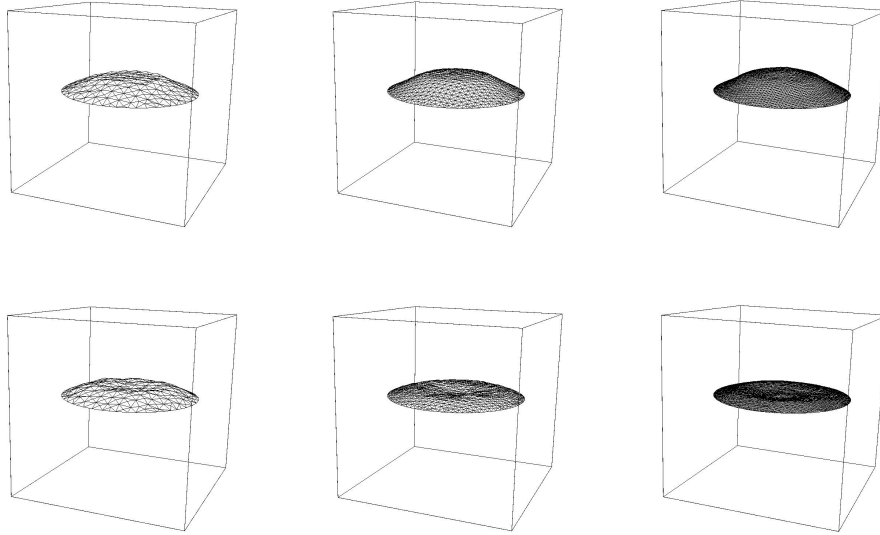


FIGURE 7. Convergence test of the drum membrane under mesh refinement. From left to right the computational mesh of the domain are 15, 30, and 60 respectively. The total mass of the membrane is kept constant in the simulations. The upper three plots show the membrane position at $t = 1$ and the lower plots show the membrane position at $t = 2$.

3.2.2. Numerical Convergence Verification. Numerical convergence under computational mesh refinement is a crucial step in assessing the validity of spring mass model. For this purpose, we carried out two sequences of simulations with increasing number of grid points. Our convergence study includes both one dimensional string in two dimensional plane and two dimensional membrane in three dimensional space.

In one case of the verification study, a circular vibrating membrane with radius of $0.4m$ and total weight of $380g$ is considered. The membrane is linearly perturbed at initial time and its circular boundary is fixed. A sequence of four cases with computational mesh 15^3 , 30^3 , 60^3 , and 120^3 are computed. The errors of total area are shown in Table 1. From Table 1, we can clearly see that the Cauchy errors are decreasing as the

reference mesh size	e_A	e_k	e_p
15 and 30	0.02528	1.91810	1.97967
30 and 60	0.01507	1.21784	1.21772
60 and 120	0.00604	0.53550	0.52837

TABLE 1. Convergence tests of spring model for a fabric drum. In the computational sequences, the total mass of the membrane is fixed. As the number of points increases, the point mass is reduced accordingly. Cauchy error is calculated on two consecutive mesh sequences. Column e_A , e_k , and e_p are errors of total area, total kinetic energy and total spring potential energy respectively. The numerical results show the first order convergence.

computational mesh is refined. The convergence rate for the membrane is also of first order.

3.2.3. *Stress Analysis.* Stress analysis on the parachute canopy and the string chords during the process of inflation is very important to the field test of the parachute. The natural stress on each side of the triangle in the spring model is the restoring force due to the stretching of each triangle side. Let τ_1, τ_2, τ_3 be the natural stress on side 1, 2, 3 of a triangle respectively, we have

$$\tau_i = k(l_i - l_i^0), \quad i = 1, 2, 3, \quad (9)$$

where k is the spring constant, l_i^0 is the equilibrium length of side i and l_i is the stretched length of the side i . This natural stress can be converted into the stress in Cartesian coordinates on the plane of the triangle. The Cartesian stress is a 2×2 tensor in the plane of the triangle

$$\sigma = \begin{pmatrix} \sigma_{xx} & \sigma_{xy} \\ \sigma_{xy} & \sigma_{yy} \end{pmatrix}. \quad (10)$$

The conversion from natural stress to Cartesian stress is through a mapping matrix, that is

$$\begin{pmatrix} \sigma_{xx} \\ \sigma_{yy} \\ \sigma_{xy} \end{pmatrix} = \begin{pmatrix} c_1^2 & s_1^2 & s_1 c_1 \\ c_2^2 & s_2^2 & s_2 c_2 \\ c_3^2 & s_3^2 & s_3 c_3 \end{pmatrix}^{-1} \begin{pmatrix} \tau_1 \\ \tau_2 \\ \tau_3 \end{pmatrix} \quad (11)$$

where $c_i = \cos \theta_i = dx_i/l_i$ and $s_i = \sin \theta_i = dy_i/l_i$ are the trig functions of the angle between each side and the x -axis. The stresses in

two principal directions are obtained via diagonalization of the stress tensor, that is

$$\begin{pmatrix} \sigma_{xx} & \sigma_{xy} \\ \sigma_{xy} & \sigma_{yy} \end{pmatrix} = T^{-1} \begin{pmatrix} \sigma_1 & 0 \\ 0 & \sigma_2 \end{pmatrix} T, \quad (12)$$

where σ_1 and σ_2 are the solutions of the characteristic equation

$$\begin{vmatrix} \sigma_{xx} - \sigma_{1,2} & \sigma_{xy} \\ \sigma_{xy} & \sigma_{yy} - \sigma_{1,2} \end{vmatrix} = 0. \quad (13)$$

We use the von Mises stress

$$\Sigma_{vm} = \sqrt{\sigma_1^2 + \sigma_2^2 - \sigma_1\sigma_2} \quad (14)$$

to measure the tension on the fabric material surface. The safety factor of the material is defined as the ratio of the significant strength of the material to the von Mises stress. When this factor is decreased to a critical value (which corresponding to high stress of the fabric surface), it sends a warning signal for the design of the parachute canopy. Figure 8 shows the von Mises stress in color in three fabric surface simulations.

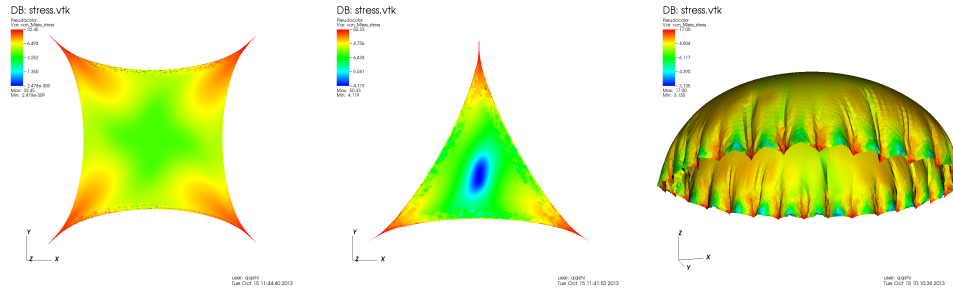


FIGURE 8. The von Mises Eq. (14) stress in the spring model. The left plot shows the von Mises stress of a rectangular membrane when pulled from the four corners. The center plot shows the von Mises stress of the triangular membrane pulled from the three vertices. The right plot is the stress on parachute canopy after inflation.

3.2.4. Fluid Canopy Coupling. To model the parachute system, an accurate coupling between the Navier-Stokes equation and the structure dynamics must be carefully considered near the canopy surface. The method we designed for the simulations of air delivery system uses the superposition of impulse on every mass point. Each mass point in the

spring system acts as an elastic boundary point and exerts an impulse on the fluid in its normal direction. Our algorithm ensures that the action and reaction between the spring mass point and the fluid solver are equal in magnitude and opposite in directions, a requirement of Newton’s third law.

We applied Peskin’s delta function immersed boundary method [18, 19]

$$\mathbf{f}(\mathbf{x}, t) = \int \mathbf{F}(s, t)\delta(\mathbf{x} - \mathbf{X}(s, t))ds. \quad (15)$$

The difference between our method and Kim and Peskin’s method lies in the calculation of \mathbf{F} . Instead of computing the tension through the derivative with respect to the arc length, we use the impulse of the mass point as a result of the superposition of three forces from the spring system, that is

$$\mathbf{F}(\mathbf{x}_i, i) = d(\mathbf{I}_g + \mathbf{I}_p + \mathbf{I}_s)/dt \quad (16)$$

Eq. (16) is more physically realistic, especially because \mathbf{I}_s is obtained from the spring equations. In the canopy spring system, we have observed that the tension is high at the top of the canopy where the curvature is almost zero.

3.2.5. Validation of the System. Our primary objective is to conduct the fabric-fluid coupled simulations and validate it against the available parachute experiments. Parachutes differ in geometry and dimensions of the canopies and risers. Among these parachutes, the T-10 parachute is used by the Army as a personnel carrier. This type of parachute has a parabolic shape for its canopy with a vent at the top. The G-11 parachute is a cargo parachute with no vent. Its dimensions could vary and is usually used as a multiple parachute system to deliver supporting equipment. We have studied the single 1/3-scale G-11 parachute inflation. The cross parachute has four open side vents and can be used as a sports parachute and small cargo carrier. Figure 9 shows the inflation sequence of a cross parachute. These three parachutes produce different patterns of airflow around the canopy and exert different drags to the parachute system.

For comparison with the indoor vertical parachute test, we initialized the parachute with flat circular canopy of 2.134 m (7 ft) nominal diameter. We carried out pre-step running to deform the parachute canopy and then used the resulting geometry as the initial state for the drop test simulation. The initial skirt diameter makes different time graph

for full inflation. In this test, there is a breathing motion or the over-inflation of the canopy. It is shown that the canopy progresses into an over-inflated shape, almost flat, and then contracts and over-inflates again. The breathing motion is an oscillatory motion. The canopy appeared to expel the excess air by means of the breathing. In the experiment, the breathing motion was also caused by the constraint on the parachute, imposed by the guide wire. The breathing motion in the simulation is smaller because there is no vertical motion restriction such as a guide wire. The terminal velocity of canopy has a good agreement with the vertical parachute test results. The experimental data shows that the descent speed rises rapidly to a peak. It slows down while the parachute inflates and then slowly approaches a steady descent speed of 4.27 m/s (14 ft/s). Even though the numerical solution cannot be compared with the experimental data during the initial period of time in the simulation, we have observed that it reaches the terminal velocity of about 3.9 m/s . The difference between the terminal velocity in numerical simulation and the experimental data is thought due to the lack of porosity of the canopy in the current numerical model. We also simulated the 1/3-scale G-11 parachute with different canopy folding level, they all converge to the terminal speed of 3 m/s in several seconds.

Parachute breathing is an oscillatory motion caused by the interaction between the fluid force and the canopy at the skirt of the parachute. The large difference between upper and lower side pressure causes vibration in the projected drag area of the canopy and thus the oscillation in descent speed. Numerical study of breathing frequency is important for understanding the stability of the parachute. In our simulation, we initialized 2.134 m (7 ft) flat-circular parachute to compare with experimental data by Tutt et al. [45]. The breathing frequency in our simulation is approximately $1.6 - 2.0 \text{ Hz}$ (0.5 s to 0.6 s period). This is in the acceptable range with the experimental frequency which is 2.0 Hz (0.5 s period). If we use a parachute with larger size or lower Reynolds number, the breathing period will increase. For example, the average period of breathing for the 10.7 m T-10 parachute is 2.3 s in experiment [10], while it is about 2 s in our simulation.

3.2.6. New Computational Development. In the last few months, we have accomplished several new tasks in the parachute simulation code which enabled us for more realistic and robust computation on the parachute problem.

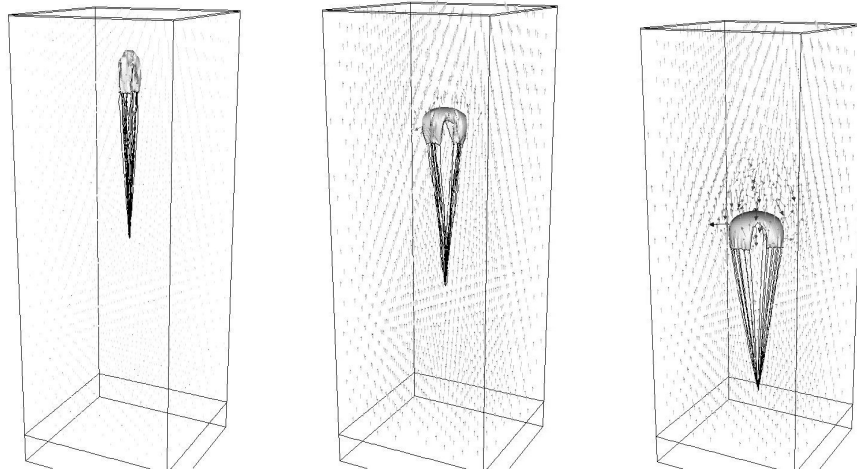


FIGURE 9. Simulation of cross parachute unfolding and inflation. The starting state of the parachute is partially folded state. The parachute has a small horizontal drift because the folded state is not perfect symmetric.

Parachute gores are stitched by the reinforcement cables. The reinforcement cables are important structures on the parachute canopy surface. To accurately model the aerodynamic motion of a parachute, we need to create a mathematical model which reveals the geometry as well as the material strength of the canopy surface and the gores. The gore structures in the parachute system have important effect on the stability of the parachute motion. In our model, we treat the reinforcement cables as curves embedded in the canopy surface. Young's modulus for the fabric surface and the reinforcement cable are set at different values. This is realized by assigning different spring constants to the surface mesh and to the gore curves. The insertion of gores as stiffened interior curves in the canopy surface mesh is demonstrated by Figure 6. Figure 10 shows that when fully inflated, the spring system reveals both the patches and the indentation of the reinforcement cables. The effect of the gores on suppressing the vortex flow at the top of the canopy is being studied. This will be published in a new paper we are currently working on.

Fabric porosity is another important property which must be correctly modeled for the canopy surface. It has long been known that fabric permeability is an important factor in parachute design. By carefully considering the balance between payload and drag, a finite

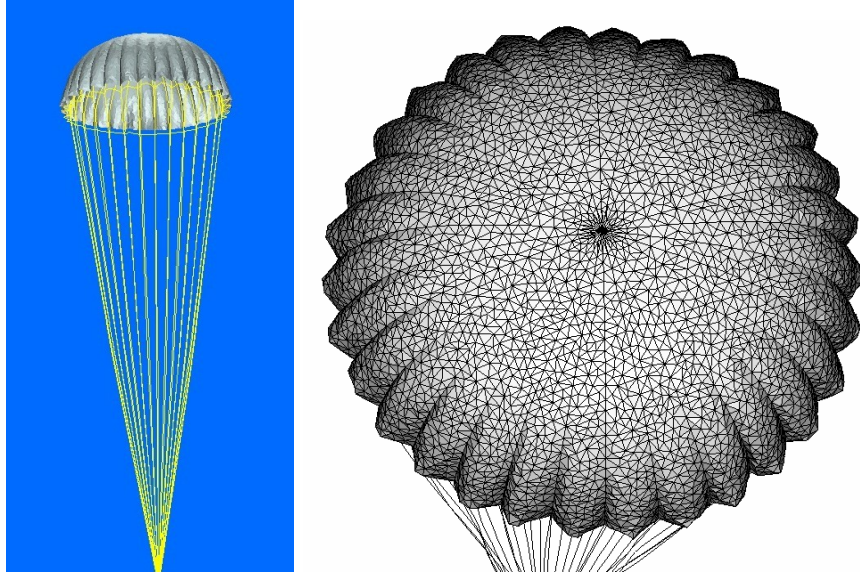


FIGURE 10. The reinforcement cables, or the gores, are modeled using the same spring system, but with different spring constant along the gore curves. The left plot shows fully opened canopy with gores. After the inflation, the gore structure is clearly revealed. The right plot shows the surface mesh and the details of the gore curves.

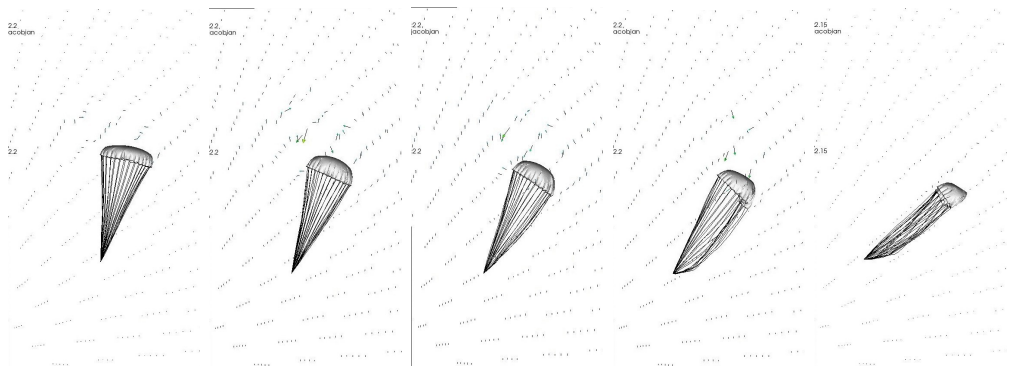


FIGURE 11. Angled deployment of C-9 parachute with the flow. The deployment angle between the initial parachute and the direction of flow are (from left to right) 15° , 30° , 45° , 60° , 75° , respectively.

permeability will make the parachute much more stable. The permeability of the parachute material often plays a vital role in the design

of parachute. A state-of-art tuning between an impervious material to a highly permeable fabric can make a parachute from a wandering sloth into a plummeting stabilizer. We have considered three different implementations of porosity for the parachute including Tezduyar and Sathe [41], Kim and Peskin [18], and Tutt[46]. We have chosen the latter two implementations because they use the similar frame work of computational mesh as we do and are easy to adapt into our front tracking environment.

For Kim and Peskin’s method, porosity is considered as the leaking pores in the immersed elastic boundary. Let β be the density of pores, which means there are βds pores in the interval $(s, s + ds)$ along the surface. If each pore has an aerodynamic conductance equal to γ , which means the flux through the pore is $\gamma(p_1 - p_2)$ where p_1 and p_2 are the pressures on the two sides of the boundary, then the flux through the interval $(s, s + ds)$ of the boundary is given by $\beta\gamma(p_1 - p_2)ds$.

Tutt’s algorithm is closest to the front tracking implementation. Tutt used the Ergun equation to describe the magnitude of porous flow velocity at a given pressure difference based on two coefficients in the following equation:

$$\frac{\Delta P}{L} = \frac{\mu}{K_1} \cdot v_f + \frac{\rho}{K_2} \cdot v_f^2 = a \cdot v_f + b \cdot v_f^2$$

where:

$$K_1 = \frac{\varepsilon^3 \cdot D^2}{150 \cdot (1 - \varepsilon)^2}$$

$$K_2 = \frac{\varepsilon^3 \cdot D}{1.75 \cdot (1 - \varepsilon)}$$

are referred to as the viscous and inertial factors respectively. D is defined as the characteristic length, ε is the porosity and is equal to the ratio of the void and total volume. v_f , μ and ρ are fluid velocity, viscosity and density respectively. In our *FronTier*-airfoil code, the pressure difference is computed after projecting the velocity into the divergence-free space. We can then use the pressure difference on two sides of the canopy to compute the v_f and add it to the advection solver as flux from the immersed elastic surface.

Collision handling on parachute contact is through the modified *FronTier* library. The computational module for parachute simulation is built on the *FronTier* library. We have used many existing data structures and functionality for geometrical handling. However, the study of parachute, airfoil and other fluid structure based simulations requires

major revisions to the software library. Among those needed are functions to handle the non-manifold surface and three dimensional curves (not as boundary of a surface, such as the string chords). The original *FronTier* code was designed for the study of fluid interface instability problems. For these problems, collision surfaces are resolved by merging or bifurcation. However, fabric surface can neither merge nor bifurcate, therefore we need to have functions which can carefully deal with the repulsive contact and collision.

Global indexing is a new feature added to the parachute code. The original *FronTier* had to deal with frequent surface mesh optimization and topological reconstructions. This makes the parallelization based on global index very difficult. As a result, the original *FronTier* library relied on floating point matching for parallel communication. The floating point matching is not 100 percent reliable and some more complicated algorithms have to be implemented as reinforcement. However for fabric surface, especially when spring model is used, the inter-connectivity and proximity of the interface marker points are not changed. Therefore, global indexing is ideal for the parallel communication of the surface. We have added a new parallel code for this functionality.

Modularization is emphasized in our code development. The parachute module is an independent application program. This new module consists of four components: (1) the initialization module, (2) the ODE module for the spring system, (3) the PDE module for fluid dynamics, and (4) the *FronTier* library for the interface geometry handling. A total of about 15,000 lines of code have been written for the first three component. An additional 4,500 lines have been added to *FronTier* to adapt the library for the computation of fabric surface.

GPU technology [20] is to use the Graphics Processing Unit (GPU) together with the CPU to accelerate a general-purpose scientific and engineering application. GPU computing can offer dramatically enhanced application performance by offloading computation-intensive portions of the programming code to the GPU units, while the remainder of the code still runs on the CPU.

Joint CPU/GPU application is a powerful combination because CPUs consist of a few cores optimized for serial processing, while GPUs consist of thousands of smaller, more efficient cores designed for massive parallel calculations. Serial portions of the code with intensive logical comparisons run on the CPU while floating point intensive parallel portions of the code run on the GPU.

3.2.7. *Delingette Modification.* Recently, Delingette [5] has studied spring model on triangulated mesh on nonlinear membrane. This new model is favored because of its derivation from the elastic membrane model in continuum mechanics.

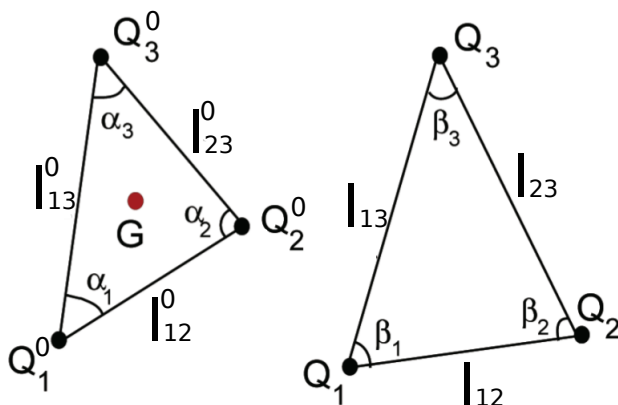


FIGURE 12. (a) Rest Triangle $T_{\mathbf{x}^0}$ whose vertices are \mathbf{x}^0_i . (b) Deformed triangle $T_{\mathbf{x}}$ whose vertices are \mathbf{x}_i

The idea of Delingette's revised model can be demonstrated by Figure 12. The energy of membrane $W(T_{\mathbf{x}^0})$ required to deform a single triangle $T_{\mathbf{x}^0}$ with vertices $\{\mathbf{x}_1^0, \mathbf{x}_2^0, \mathbf{x}_3^0\}$ into its deformed position $T_{\mathbf{x}}$ with vertices $\{\mathbf{x}_1, \mathbf{x}_2, \mathbf{x}_3\}$ consists of two parts,

- The energy of three tensile springs that prevent edges from stretching.
- The energy of three angular springs that prevent any change of vertex angles.

We use $A_{\mathbf{x}^0}$, α_i and l_{ij}^0 to represent the initial area, initial angles and initial lengths of the rest triangle $T_{\mathbf{x}^0}$. Correspondingly, we use $A_{\mathbf{x}}$, β_i and l_{ij} to denote the area, angles, and lengths of the deformed triangle $T_{\mathbf{x}}$. The edge elongation can be written as $dl_{ij} = l_{ij} - l_{ij}^0$. Based on the analysis by Delingette [5], we have

$$W(T_{\mathbf{x}^0}) = \sum_{i=1}^3 \frac{1}{2} k_i^{T_{\mathbf{x}^0}} (dl_{jk})^2 + \sum_{i \neq j} \gamma_k^{T_{\mathbf{x}^0}} dl_{ik} dl_{jk}$$

where

$$k_i^{T_{\mathbf{x}^0}} = \frac{(l_{jk}^0)^2 (2 \cot^2 \alpha_i (\lambda + \mu) + \mu)}{8A_{\mathbf{x}^0}}$$

is the tensile stiffness and

$$\gamma_k^{T_{\mathbf{x}^0}} = \frac{l_{ik}^0 l_{jk}^0 (2 \cot \alpha_i \cot \alpha_j (\lambda + \mu) - \mu)}{8A_{\mathbf{x}^0}}$$

is the angular stiffness. γ and μ are the lame coefficients of the material. Those coefficients are simply related to the two physically meaningful parameters defined in planar elasticity for a membrane, that is, the Young modulus E and the Poisson coefficient ν [6]:

$$\lambda = \frac{E\nu}{1-\nu^2} \text{ and } \mu = \frac{E(1-\nu)}{1-\nu^2}.$$

The Young modulus quantifies the stiffness of the material, whereas the Poisson coefficient characterizes the material compressibility.

Applying the Rayleigh-Ritz analysis, it is considered that the fabric surface represented by triangular mesh should evolve by minimizing its membrane energy, therefore along the opposite derivative of that energy with respect to the nodes of the system, that is, the deformed positions \mathbf{x}_i :

$$\begin{aligned} F_i(T_{\mathbf{x}^0}) &= -\frac{\partial W(T_{\mathbf{x}^0})}{\partial \mathbf{x}_i} \\ &= \sum_{j \neq i} k_j^{T_{\mathbf{x}^0}} (dl_{ik}) \frac{\mathbf{x}_k - \mathbf{x}_i}{l_{ik}} + \sum_{j \neq i} (\gamma_k^{T_{\mathbf{x}^0}} dl_{jk} + \gamma_i^{T_{\mathbf{x}^0}} dl_{ij}) \frac{\mathbf{x}_k - \mathbf{x}_i}{l_{ik}} \end{aligned} \quad (17)$$

The membrane energy to deform the whole triangulation is simply the sum of the energy of each triangle. Thus, if an edge is shared by two triangles T_1 and T_2 , the total stiffness of that edge k^T is the sum of the two stiffness coefficients: $k^T = k^{T_1} + k^{T_2}$.

If the second term in Eq. (17) is neglected, Delingette's model is the same as our original model except that the spring constant will vary if the corresponding initial triangle deviate from the isosceles triangle.

3.3. Turbulence Modeling.

3.3.1. *Theory.* We exploited systematically the K41 theory of turbulence. This description of the velocity statistics is in effect a Sobolev inequality, and assuming this, we derive an existence theorem, not just for the Navier-Stokes equation, but for the limiting infinite Reynolds number Euler equation [3]. Pursuing this same set of scaling ideas, we interpreted the derivation of subgrid terms in terms of the renormalization group, with higher order corrections [7]. Perhaps the most

important idea to emerge from this line of reasoning is a clear picture of physically based nonuniqueness of solutions for the LES turbulence and turbulence mixing simulations and for the limiting Euler equations (whose solution we just established). The idea is that the compressible Euler equation and the multifluid Euler equation (compressible or not) have dimensionless parameters related to the Schmidt and Prandtl numbers and to the ratio of the bulk to shear viscosity. For LES simulations, the parameters have turbulent versions, not specified by laws of physics, but rather by the requirement that the coarse grid simulations should converge as best as possible to highly resolved (infinite Reynolds number) simulations. Since the latter can not be achieved in practice, the requirement is in effect unspecified, and is only settled by comparison to experiment. These parameters introduce nonuniqueness to the LES solutions. This is in some sense a crisis for applied computational science, which generally believes that a numerically correct simulation will give rise to a physically correct answer. We see that this statement is only asymptotically correct in the limit of infinite mesh resolution, that is for direct numerical simulations. To repair this crisis, we introduced a validation program, which was quite successful, relative to the range of experimental data. The fluid mixing data set runs up to $Re = 35,000$, but many important problems arise at higher Reynolds numbers. For this regime, we demonstrated that a numerical extrapolation from the experimental Reynolds numbers to much higher ones is quite mild, so that effective validation, with a mild layer of extrapolation, i.e., verification, will suffice [24, 25].

In current and ongoing work we have begun the extension of these results to the convergence of the cumulative distribution functions (the first integral of the probability density functions). A statistical tool, called W^* , was developed to assist in the statistical data analysis, for this modified notion of stochastic convergence [17].

The stochastic convergence was demonstrated in a series of papers [14, 15, 22], and continues with our current research. See Figs. 13 and 14.

3.3.2. *Simulations.* [8, 11] [12] [13] The observation of Sec. 3.3.1 that turbulent mixing simulations and all but the simplest (incompressible, constant density single fluid) LES turbulent simulations are physically underspecified and possess nonunique solutions has profound implications for numerical simulations. Even this one exceptional case has been shown to have nonunique solutions in a mathematical analysis.

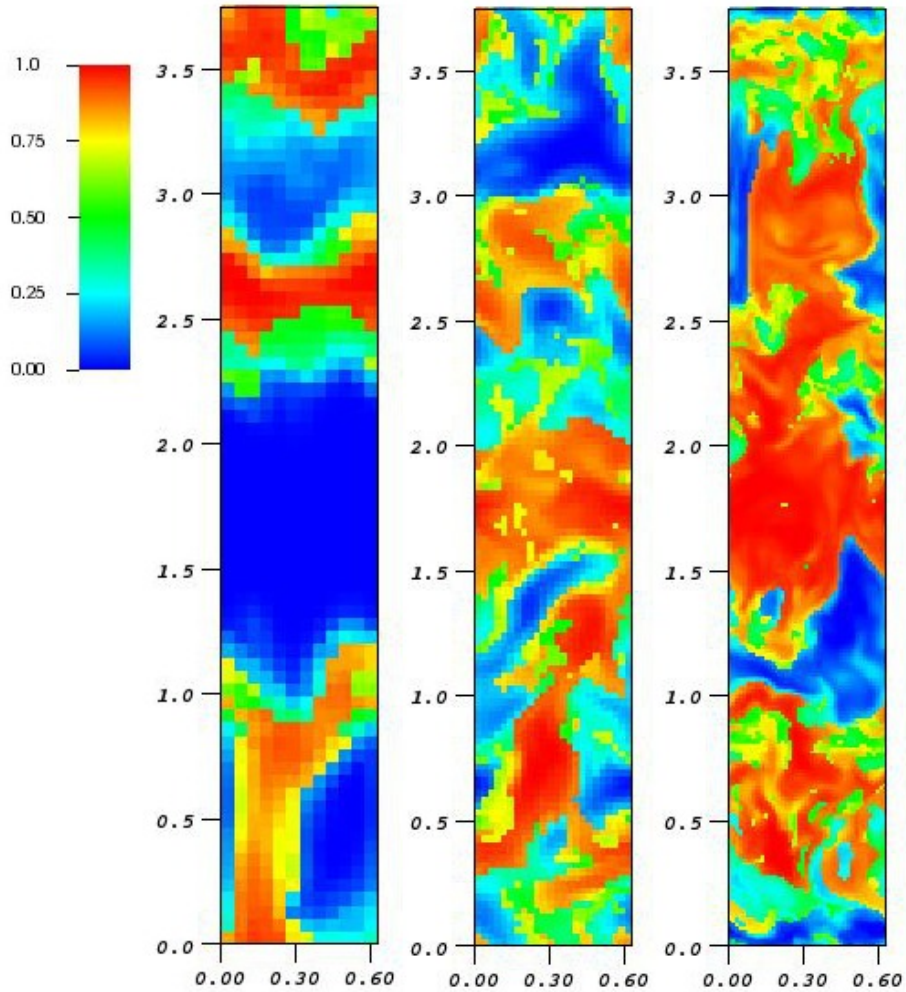


FIGURE 13. Species concentration in a fluid mixture taken in a slice through the middle of the mixing zone. Left to right: coarse, medium and fine grids. Visual inspection suggests some kind of mesh convergence of the mixture fractions, from a statistical point of view. See Fig. 14 for a quantitative measure of this convergence.

Because of the nonuniqueness, verification, that is convergence under mesh refinement, is insufficient to assure physically correct answers. Validation, that is comparison to experiment, is essential for scientific accuracy. Fortunately, the algorithm we developed, Front Tracking combined with subgrid scale terms (FT/SGS) gives basically exact results compared to experiment for LES turbulent mixing [8, 11]. See Fig. 16 for an example of solution validation. These two ingredients,

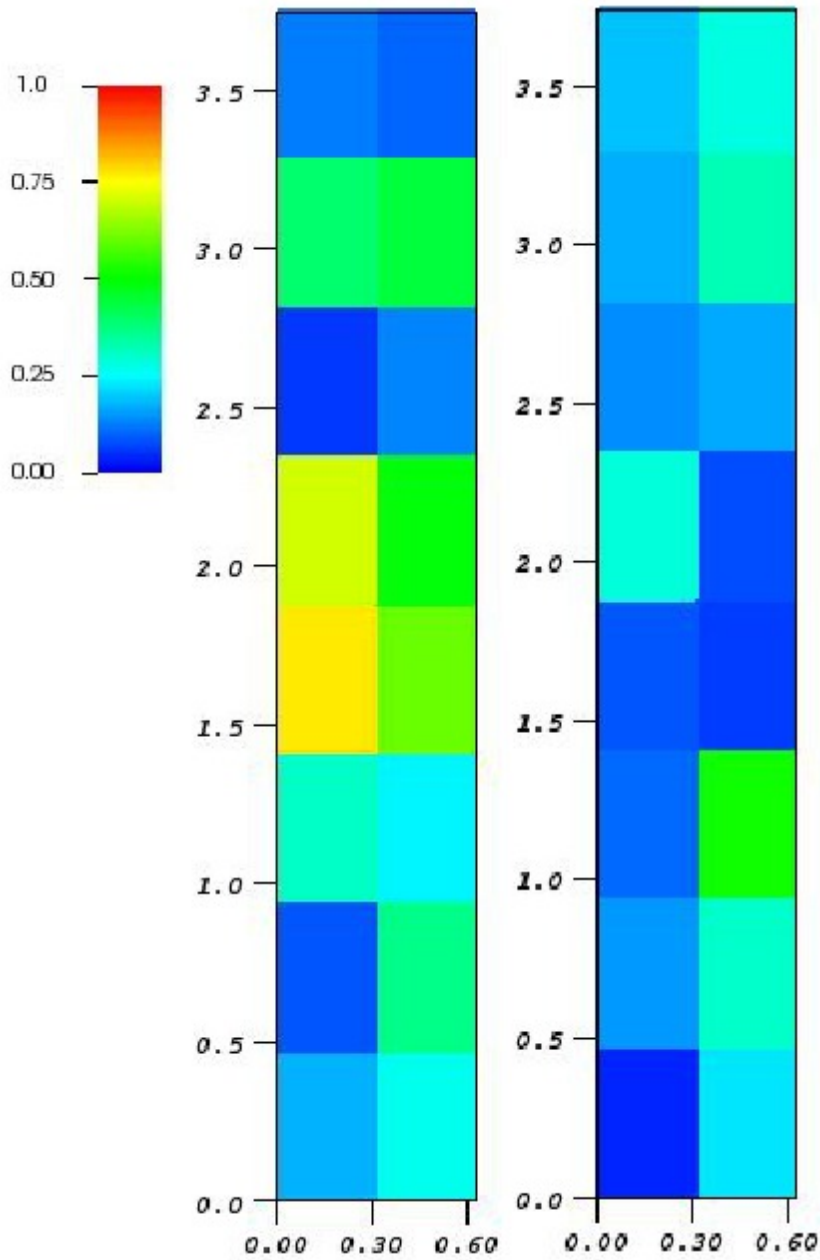


FIGURE 14. L_1 norm differences of the cumulative distribution functions, from the concentrations shown in Fig. 13. The two plots compare coarse to fine (left) and medium to fine (right). The decrease error measured in the L_1 norm under mesh refinement is a quantitative measure of the stochastic convergence.

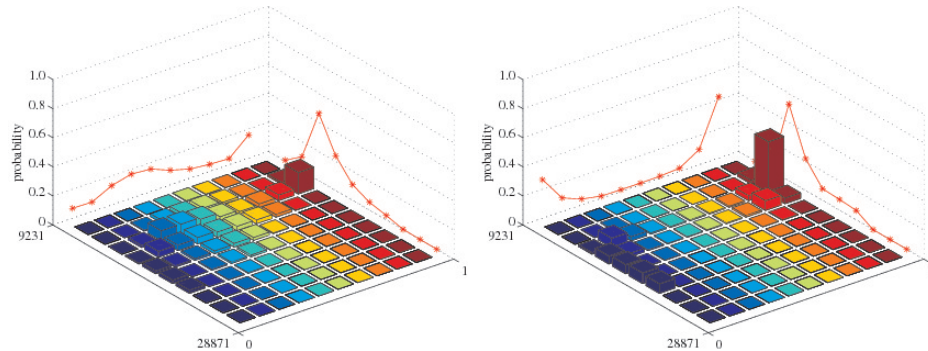


FIGURE 15. LES simulations for a shock wave induced mixing problem using two different choices of the sub-grid model coefficients. The difference in the solutions indicates the nonuniqueness of the simulation.

tracking and subgrid models, play different and opposite roles. The SGS terms add turbulent diffusion and viscosity, while the front tracking prevents excess thermal and species diffusion. We believe that any good numerical scheme with both of these elements will obtain a nearly correct answer. However, final tuning to account for algorithm dependent changes still leads to required adjustments to achieve validation goals. The tuning will amount to adjustment of diffusion terms [24].

In Fig. 15, we show the probability density functions from two simulations of a shock driven turbulent mixing simulation, but with different subgrid model coefficients. The disparity of the solutions is a numerical confirmation of nonuniqueness.

Uncertainty quantification was addressed in these studies. Our validation studies concern the edge of the mixing zone for Rayleigh-Taylor instabilities. Unmeasured long wave lengths in the initial conditions were assessed from early time experimental plates, and reconstructed, with quantified uncertainty, leading to an overall uncertainty in the final experimental value of $\pm 5\%$ [8, 11], see Fig. 16.

Current and future work will focus on the convergence of the probability distribution functions for the mixtures. Initial results show evidence of such convergence for the first integral of the pdfs, namely the cumulative distribution functions [25, 13]; These same references display evidence for the nonuniqueness of the solutions as the SGS terms (or equivalently the algorithm) are varied.

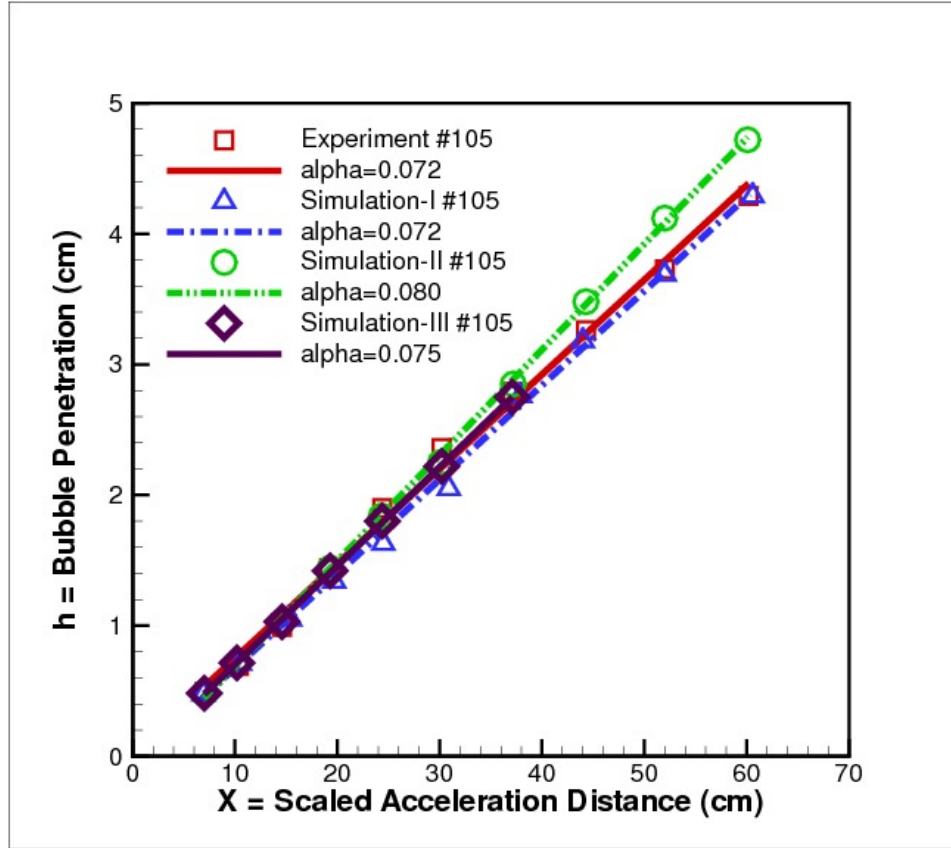


FIGURE 16. A comparison study of three simulations and experimental data points, for an acceleration driven fluid instability problem. The three simulations have the nominal long wave length (reconstructed from experiment) initial conditions, and the same multiplied by 0 or 2, with this (large) margin set from uncertainties in the methods of data analysis. The observed variation of the instability growth rate is $\pm 5\%$.

3.3.3. *Tech Transfer.* **LANL** We simulate turbulent mixing in inertial confinement flows. As a base calculation, we find simulation models which show improved fit to experimental data. These models will be used to test the turbulent mixing and stochastic convergence models developed here, in an A B comparison (with and without enhanced resolution methods).

ORNL We study a highly agitated two phase flow designed to enhance chemical reactions occurring at the interface between the two phases [23]. A correction to the Navier-Stokes equation, an added pressure,

called disjuncture pressure a surface effect similar in origin to surface tension)) is needed to capture experimentally observed small phenomena of local phase separation. The extra pressure is a surface related force familiar in lubrication theory, and has an origin in thermodynamics similar to that of surface tension. It retards the merging of bubbles embedded in the two phase flow and greatly enhances the surface area, thereby accelerating the chemical reactions.

Stanford University We study turbulent combustion in the engine of a scram jet. The main thrust of the effort was to develop finite rate chemistry simulation models. We also study interaction of turbulence, particle laden flow and radiation. Depending on the Stokes number, the particles cluster in narrow regions of high strain rate, exterior to vortex tubes.

4. IMPACT TO EDUCATION AND TRAINING

The previous research grant also supported Joungdong Kim, a permanent resident of the United States. Parachute simulation is the main topic of Dr. Kim's PhD thesis. After graduation, Joungdong Kim joined the Mathematics Department of University of Texas A&M as a visiting assistant professor. Another former student from our research group, Eric Rathnayke joined Military Accessions Vital to the National Interest (MAVNI) program this year. A new student, Bernard Moore joined our group in the spring. He participated the US Air Force SFFP program and is highly motivated by our project as well as the service to the military. The numerical techniques we studied so far have had an impact on education and training. In the previous project, we recruited and advised three high school students for their summer research in computational simulation of parachute and other fluid-structure interactions. These students were Andrew Ahn and Thomas Hobbs from the Ward Melville High School, and Heisler, Alicia from North Shore Hebrew Academy High School.

- [1] I. BOLOTNOV, F. BEHAFARID, D. SHAVER, T. GUO, S. WANG, H. WEI, , S. ANTHAL, K. JANSEN, R. SAMULYAK, AND M. PODOWSKI, *Interaction of computational tools for multi-scale multiphysics simulations of generation-iv reactors*, in Proceedings of ICAPP 2010, San Diego, CA, June 13-17, 2010, p. Paper 10141.
- [2] I. BOLOTNOV, F. BEHAFARID, D. SHAVER, H. HEI, S. ANTHAL, K. JANSEN, R. SAMULYAK, H. WEI, AND M. PODOWSKI, *Multiscale computer simulations of fission gas discharge during loss-of-flow accident in sodium fast reactor*, in OECD Nuclear Energy Agency and IAEA Workshop (CFD4NRS-3) on Experimental Validation and Application of CFD and CMFD Codes to Nuclear Reactor Safety Issues, Washington D.C., September 14-16, 2010.
- [3] G.-Q. CHEN AND J. GLIMM, *Kolmogorov's theory of turbulence and inviscid limit of the Navier-Stokes equations in R^3* , Commun. Math. Phys., 310 (2012), pp. 267-283.

- [4] B. CLARK, N. RAY, AND X. JIAO, *Surface mesh optimization, adaption and untangling with high-order accuracy*, 21st International Meshing Roundtable, (2012).
- [5] H. DELINGETTE, *Triangular springs for modeling nonlinear membranes*, IEEE Transactions on Visualization and Computer Graphics Volume 14 Issue 2, (2008).
- [6] J. M. GERE, *Mechanics of materials, sixth edition*, Bill Stenquist, 2004.
- [7] J. GLIMM, B. PLOHR, AND D. SHARP, *Large eddy simulation, turbulent transport and the renormalization group*, arXiv, arxiv.org ζ physics.flu-dyn ζ 1308.3221 (2013). Los Alamos National Laboratory Preprint Number LA-UR-12-26149, Stony Brook University Preprint Number SUNYSB-AMS-12-02.
- [8] J. GLIMM, D. H. SHARP, T. KAMAN, AND H. LIM, *New directions for Rayleigh-Taylor mixing*, Phil. Trans. R. Soc. A, 371 (2013), p. 20120183. Los Alamos National Laboratory Preprint LA-UR 11-00423 and Stony Brook University Preprint SUNYSB-AMS-11-01.
- [9] X. JIAO AND D. WANG, *Reconstructing high-order surfaces for meshing*, Engineering with Computers, 28 (2012), pp. 361–373.
- [10] H. JOHARI AND K. J. DESABRAIS, *Vortex shedding in the near wake of a parachute canopy*, J. Fluid Mech., 536 (2005), pp. 185–207.
- [11] T. KAMAN, J. GLIMM, AND D. H. SHARP, *Initial conditions for turbulent mixing simulations*, Condensed Matter Physics, 13 (2010), p. 43401. Stony Brook University Preprint number SUNYSB-AMS-10-03 and Los Alamos National Laboratory Preprint number LA-UR 10-03424.
- [12] ———, *Uncertainty quantification for turbulent mixing simulation*, 5th International Conference of Numerical Modeling of Space Plasma Flows (ASTRONUM 2010), 444 (2010), p. 21. Stony Brook University Preprint number SUNYSB-AMS-10-04. Los Alamos National Laboratory preprint LA-UR 11-00422.
- [13] T. KAMAN, R. KAUFMAN, J. GLIMM, AND D. H. SHARP, *Uncertainty quantification for turbulent mixing flows: Rayleigh-Taylor instability*, in Uncertainty Quantification in Scientific Computing, A. Dienstfrey and R. Boisvert, eds., vol. 377 of IFIP Advances in Information and Communication Technology, Springer, 2012, pp. 212–225. Stony Brook University Preprint number SUNYSB-AMS-11-08.
- [14] T. KAMAN, H. LIM, Y. YU, D. WANG, Y. HU, J.-D. KIM, Y. LI, L. WU, J. GLIMM, X. JIAO, X.-L. LI, AND R. SAMULYAK, *A numerical method for the simulation of turbulent mixing and its basis in mathematical theory*, in Lecture Notes on Numerical Methods for Hyperbolic Equations: Theory and Applications: Short Course Book, CRC/Balkema, London, 2011, pp. 105–129. Stony Brook University Preprint SUNYSB-AMS-11-02.
- [15] T. KAMAN, J. MELVIN, P. RAO, R. KAUFMAN, H. LIM, Y. YU, J. GLIMM, AND D. H. SHARP, *Recent progress in turbulent mixing*, Physica Scripta, (2013), p. 014051. Stony Brook University Preprint number SUNYSB-AMS-11-09. Los Alamos National Laboratory preprint LA-UR 11-06770.
- [16] K. KARAGIOZIS, R. KAMAKOTI, F. CIRAK, AND C. PANTANO, *A computational study of supersonic disk-gap-band parachutes using large-eddy simulation coupled to a structural membrane*, Journal of Fluids and Structures, 27 (2011), pp. 175–192.
- [17] R. KAUFMAN, T. KAMAN, Y. YU, AND J. GLIMM, *Stochastic convergence and the software tool W^** , in Proceeding Book of International Conference to honour Professor E.F. Toro, CRC, Taylor and Francis Group, 2012, pp. 37–41. Stony Brook University Preprint number SUNYSB-AMS-11-10.
- [18] Y. KIM AND C. S. PESKIN, *2-D parachute simulation by the immersed boundary method*, SIAM J. Sci. Comput., 28 (2006), pp. 2294–2312.

- [19] ———, *3-D parachute simulation by the immersed boundary method*, *Comput. Fluids*, 38 (2009), pp. 1080–1090.
- [20] D. B. KIRK AND W. H. WEN-MEI, *Programming massively parallel processors: a hands-on approach*, Morgan Kaufmann, 2010.
- [21] Y. LI, I.-L. CHERN, J.-D. KIM, AND X.-L. LI, *Numerical method of fabric dynamics using front tracking and spring model*, *Communications in Computational Physics*, (2012). Submitted.
- [22] H. LIM, T. KAMAN, Y. YU, V. MAHADEO, Y. XU, H. ZHANG, J. GLIMM, S. DUTTA, D. H. SHARP, AND B. PLOHR, *A mathematical theory for LES convergence*, *Acta Mathematica Scientia*, 32 (2012), pp. 237–258. Stony Brook University Preprint SUNYSB-AMS-11-07 and Los Alamos National Laboratory Preprint LA-UR 11-05862.
- [23] H. K. LIM, Y. ZHOU, V. F. DE ALMEIDA, AND J. GLIMM, *Fully developed turbulent mixing in an annular sector*, *HYP2012 Proceedings*, (2012). Submitted for publication, Stony Brook University Preprint Number SUNYSB-AMS-12-03.
- [24] J. MELVIN, R. KAUFMAN, H. LIM, T. KAMAN, P. RAO, AND J. GLIMM, *Macro and micro issues in turbulent mixing*, *Science China Technological Sciences*, (2013), pp. 1–6.
- [25] J. MELVIN, P. RAO, R. KAUFMAN, H. LIM, Y. YU, J. GLIMM, AND D. H. SHARP, *Atomic scale mixing for inertial confinement fusion associated hydro instabilities*, *High Energy Density Physics*, 9 (2013), pp. 288–298. Stony Brook University Preprint SUNYSB-AMS-12-01 and Los Alamos National Laboratory Preprint LA-UR 12-21555.
- [26] J. W. PURVIS, *Prediction of line sail during lines-first deployment*, *AIAA 21st Aerospace Sciences Meeting*, (1983).
- [27] ———, *Numerical prediction of deployment, initial fill, and inflation of parachute canopies*, *8th AIAA Aerodynamic Decelerator and Balloon Technology Conference*, (1984).
- [28] N. RAY, T. DELANEY, D. EINSTEIN, AND X. JIAO, *Surface remeshing with robust high order reconstruction*, *Engineering with Computers*, (2013). submitted.
- [29] N. RAY, D. WANG, X. JIAO, AND J. GLIMM, *High-order numerical integration over discrete surfaces*, *SIAM Journal on Numerical Analysis*, 50 (2012), pp. 3061–3083.
- [30] K. STEIN, R. BENNEY, V. KALRO, T. E. TEZDUYAR, J. LEONARD, AND M. ACCORSI, *Parachute fluid-structure interactions: 3-D computation*, *Comput. Methods Appl. Mech. Engrg*, 190 (2000), pp. 373–386.
- [31] K. STEIN, R. BENNEY, T. TEZDUYAR, AND J. POTVIN, *Fluid-structure interactions of a cross parachute: numerical simulation*, *Computer Methods in Applied Mechanics and Engineering*, 191 (2001), pp. 673–687.
- [32] K. STEIN, T. TEZDUYAR, V. KUMAR, S. SATHE, R. BENNEY, E. THORNBURG, C. KYLE, AND T. NONOSHITA, *Aerodynamic interactions between parachute canopies*, *J. Appl. Mech.*, 70 (2003), pp. 50–57.
- [33] K. R. STEIN, R. J. BENNEY, V. KALRO, A. A. JOHNSON, AND T. E. TEZDUYAR, *Parallel computation of parachute fluid-structure interactions*, *14th Aerodynamic Decelerator Systems Technology Conference*, (1997).
- [34] K. R. STEIN, R. J. BENNEY, E. C. STEEVES, D. U.S. ARMY NATICK RESEARCH, AND E. CENTER, *A computational model that couples aerodynamic and structural dynamic behavior of parachutes during the opening process*, *Technical report (U.S. Army Natick Laboratories)*, United States Army Natick Research, Development and Engineering Center, Aero-Mechanical Engineering Directorate, 1993.

- [35] K. R. STEIN, R. J. BENNEY, T. E. TEZDUYAR, J. W. LEONARD, AND M. L. ACCORSI, *Fluid-structure interactions of a round parachute: Modeling and simulation techniques*, J. Aircraft, 38 (2001), pp. 800–808.
- [36] J. H. STRICKLAND, V. L. PORTER, G. F. HOMICZ, AND A. A. GOSSLER, *Fluid-structure coupling for lightweight flexible bodies*, 17th AIAA Aerodynamic Decelerator Systems Technology Conference and Seminar, (2003).
- [37] K. TAKIZAWA, C. MOORMAN, S. WRIGHT, T. SPIELMAN, AND T. E. TEZDUYAR, *Fluid-structure interaction modeling and performance analysis of the orion spacecraft parachutes*, International Journal for Numerical Methods in Fluids, 65 (2011), pp. 271–285.
- [38] K. TAKIZAWA, T. SPIELMAN, AND T. E. TEZDUYAR, *Space-time FSI modeling and dynamical analysis of spacecraft parachutes and parachute clusters*, Computational Mechanics, 48 (2011), pp. 345–364.
- [39] T. TEZDUYAR, M. BEHR, AND J. LIOU, *A new strategy for finite element computations involving moving boundaries and interfaces: the deforming-spatial-domain/space-time procedure: I. the concept and the preliminary numerical tests*, Computer Methods in Applied Mechanics and Engineering, 94 (1992), pp. 339 – 351.
- [40] T. TEZDUYAR, M. BEHR, S. MITTAL, AND J. LIOU, *A new strategy for finite element computations involving moving boundaries and interfaces: the deforming-spatial-domain/space-time procedure: II. computation of free-surface flows, two-liquid flows, and flows with drifting cylinders*, Computer Methods in Applied Mechanics and Engineering, 94 (1992), pp. 353 – 371.
- [41] T. E. TEZDUYAR AND S. SATHE, *Modelling of fluid-structure interactions with the space-time finite elements: Solution techniques*, International Journal for Numerical Methods in Fluids, 54 (2007), pp. 855–900.
- [42] T. E. TEZDUYAR, S. SATHE, R. KEEDY, AND K. STEIN, *Space-time finite element techniques for computation of fluid-structure interactions*, Computer Methods in Applied Mechanics and Engineering, 195 (2006), pp. 2002–2027.
- [43] T. E. TEZDUYAR, S. SATHE, M. SCHWAAB, J. PAUSEWANG, J. CHRISTOPHER, AND J. CRABTREE, *Fluid-structure interaction modeling of ringsail parachutes*, Computational Mechanics, 43 (2008), pp. 133–142.
- [44] T. E. TEZDUYAR, K. TAKIZAWA, C. MOORMAN, S. WRIGHT, AND J. CHRISTOPHER, *Space-time finite element computation of complex fluid-structure interactions*, International Journal for Numerical Methods in Fluids, 64 (2010), pp. 1201–1218.
- [45] B. TUTT, S. ROLAND, R. D. CHARLES, AND G. NOETSCHER, *Finite mass simulation techniques in LS-DYNA*, 21st AIAA Aerodynamic Decelerator Systems Technology Conference and Seminar, (2011).
- [46] B. A. TUTT AND A. P. TAYLOR, *The use of LS-DYNA to simulate the inflation of a parachute canopy*, 18st AIAA Aerodynamic Decelerator Systems Technology conference and Seminar, (2005).
- [47] D. WANG, X. JIAO, R. CONLEY, AND J. GLIMM, *On the curvature effect of thin membranes*, J. Comput. Phys., (2012). Accepted.
- [48] H. WEI, *Mesoscale Models and Numerical Algorithms for Fracture of Solids*, Ph.D. Thesis, Stony Brook University, 2012.
- [49] R. S. H. WEI, *Mesoscale models for fracture of brittle materials*, in Proceedings of the ASME Applied Mechanics and Materials Conference, May 30 - June 1, 2011.